



**HAL**  
open science

## **cIAP1/TRAF2 interplay promotes tumor growth through the activation of STAT3**

Baptiste Dumétier, Aymeric Zadoroznyj, Jean Berthelet, Sébastien Causse,  
Jennifer Allègre, Pauline Bourgeois, Florine Cattin, Cindy Racœur, Catherine  
Paul, Carmen Garrido, et al.

► **To cite this version:**

Baptiste Dumétier, Aymeric Zadoroznyj, Jean Berthelet, Sébastien Causse, Jennifer Allègre, et al..  
cIAP1/TRAF2 interplay promotes tumor growth through the activation of STAT3. *Oncogene*, In  
press, 10.1038/s41388-022-02544-y . hal-03882909

**HAL Id: hal-03882909**

**<https://hal.science/hal-03882909>**

Submitted on 2 Dec 2022

**HAL** is a multi-disciplinary open access archive for the deposit and dissemination of scientific research documents, whether they are published or not. The documents may come from teaching and research institutions in France or abroad, or from public or private research centers.

L'archive ouverte pluridisciplinaire **HAL**, est destinée au dépôt et à la diffusion de documents scientifiques de niveau recherche, publiés ou non, émanant des établissements d'enseignement et de recherche français ou étrangers, des laboratoires publics ou privés.

1 **clAP1/TRAF2 interplay promotes tumor growth through the activation of STAT3.**

2 Baptiste Dumétier<sup>1,2\*</sup>, Aymeric Zadoroznyj<sup>1,2\*</sup>, Jean Berthelet<sup>1,2,a</sup>, Sebastien Causse<sup>1,2</sup>, Jennifer Allègre<sup>1,2</sup>, Pauline  
3 Bourgeois<sup>1,2</sup>, Florine Cattin<sup>1,2</sup>, Cindy Racœur<sup>3,4</sup>, Catherine Paul<sup>3,4</sup>, Carmen Garrido<sup>1,2,5</sup>, Laurence Dubrez<sup>1,2</sup>.

4  
5  
6  
7  
8 <sup>1</sup> Institut National de la Santé et de la Recherche Médicale (Inserm), LNC UMR1231, LabEx LlpSTIC, 21000 Dijon,  
9 France; Team with the label of excellence from « la ligue national contre le Cancer »

10 <sup>2</sup> Université de Bourgogne-Franche-Comté, 21000 Dijon, France

11 <sup>a</sup> Current address: Olivia Newton-John Cancer Research Institute, Heidelberg, Victoria, Australia

12 <sup>3</sup> LIIC, EA7269, Université de Bourgogne-Franche-Comté, 21000 Paris, France.

13 <sup>4</sup> Laboratory of Immunology and Immunotherapy of Cancers, EPHE, PSL Research University, 75000 Paris, France.

14 <sup>5</sup> Anticancer Center Georges François Leclerc-Unicancer, Dijon, France

15 \* these authors contributed equally to this work

16 Correspondence: ldubrez@u-bourgogne.fr  
17

18  
19  
20 **Running title:** clAP1-TRAF2 interplay in tumor growth  
21

22 **Statement of Significance:** clAP1/TRAF2 complexes regulates the JAK/STAT3 signaling pathway, which is critical for  
23 the tumor-promoting activity of clAP1.  
24

25 **Keywords:** clAP1/oncogene/STAT3/TRAF2.

26 Data Availability statement: Figshare DOI <https://doi.org/10.6084/m9.figshare.21399906>

27 **Competing Interests:** The authors declare no competing financial interests  
28

29 **Abstract**

30

31 Cellular inhibitor of apoptosis-1 (cIAP1) is a signaling regulator with oncogenic properties. It is involved in the  
32 regulation of signaling pathways controlling inflammation, cell survival, proliferation, differentiation and motility. It is  
33 recruited into membrane-receptor associated signaling complexes thanks to the molecular adaptor TRAF2. However,  
34 the cIAP1/TRAF2 complex exists, independently of receptor engagement, in several subcellular compartments. The  
35 present work strengthens the importance of TRAF2 in the oncogenic properties of cIAP1. cIAPs-deficient mouse  
36 embryonic fibroblasts (MEFs) were transformed using the HRas-V12 oncogene. Re-expression of cIAP1 enhanced  
37 tumor growth in a nude mice xenograft model, and promoted lung tumor nodes formation. Deletion or mutation of  
38 the TRAF2-binding site completely abolished the oncogenic properties of cIAP1. Further, cIAP1 mediated the clustering  
39 of TRAF2, which was sufficient to stimulate tumor growth. Our TRAF2 interactome analysis showed that cIAP1 was  
40 critical for TRAF2 to bind to its protein partners. Thus, cIAP1 and TRAF2 would be two essential subunits of a signaling  
41 complex promoting a pro-tumoral signal. cIAP1/TRAF2 promoted the activation of the canonical NF- $\kappa$ B and ERK1/2  
42 signaling pathways. NF- $\kappa$ B-dependent production of IL-6 triggered the activation of the JAK/STAT3 axis in an autocrine  
43 manner. Inhibition or downregulation of STAT3 specifically compromised the growth of cIAP1-restored MEFs but not  
44 that of MEFs expressing a cIAP1-mutant and treating mice with the STAT3 inhibitor niclosamide completely abrogated  
45 cIAP1/TRAF2-mediated tumor growth. Altogether, we demonstrate that cIAP1/TRAF2 binding is essential to promote  
46 tumor growth via the activation of the JAK/STAT3 signaling pathway.

47

48

49

50

51

52

## 53 Introduction

54

55 Cellular Inhibitors of apoptosis 1 and 2 (cIAP1/2) and tumor necrosis factor-associated factors 2 (TRAF2) were purified  
56 together in 1995 by Rothe *et al.* in a pull-down experiment aiming to identify cytoplasmic components of the tumor  
57 necrosis factor receptor-2 (TNFR2) complex (1). cIAP1/2 are RING containing-E3-ubiquitin ligases belonging to the  
58 IAP (Inhibitor of apoptosis) family (2). They catalyze the conjugation of ubiquitin chains of different topologies  
59 including K6-, K11-, K27-, K48- and K63-linked chains resulting in modification of the stability, activity or interaction  
60 network of protein substrates. Their ubiquitination substrates are specifically recruited thanks to the presence of three  
61 conserved protein-protein interacting domains named BIRs (Baculoviral IAP repeats) at the N-terminal extremity.  
62 More than thirty substrates have been identified so far (3). They comprise cell death regulators such as the IAP  
63 antagonist Smac, cell signaling intermediates including receptor-interacting kinases (RIPs), NF- $\kappa$ B-inducing kinase (NIK)  
64 and raf proto-oncogene serine/threonine protein kinase (Raf1), regulators of cellular architecture such as some  
65 GTPases from the Rho family and transcription factors including E2F1, the Interferon Regulatory Factor 1 (IRF1) and  
66 the C/EBP homologous protein (CHOP) (for a review, see(3)). Thus, cIAPs have been involved in the regulation of  
67 inflammation, cell differentiation, cell death, cell proliferation and cell migration. cIAP1 is more strongly expressed  
68 than cIAP2 in most tissues, except in bone marrow and lymphoid tissues in which cIAP2 is predominant (4). Consistent  
69 with its functions in promoting cell survival and proliferation, oncogenic properties of cIAP1 have been demonstrated  
70 in several mouse models (5-7).

71

72 As cIAP1, TRAF2 is a RING-containing protein. However, its E3-ligase activity seems relatively weak (8, 9). It is  
73 considered as a molecular adaptor bridging signaling molecules to receptors (10). It can directly or indirectly bind  
74 certain members of TNFR including TNFR1, TNFR2, CD30, CD40 and B-cell activating factor (BAFF-R), toll-like receptor-  
75 4 (TLR4), some nucleotide binding-oligomerization domain (NOD)-like receptors (NLRs), retinoic acid-inducible gene I  
76 (RIG-1)-like receptors (RLRs) and some cytokine receptors (10). TRAF2 serves as an intermediate for the recruitment  
77 of cIAPs into receptor-associated complexes. However, the cIAP1-TRAF2 complex has also been observed in the  
78 cytoplasm as well as in the nucleus, independently of receptor engagement (8, 11-14).

79 Here, by using HRas-V12-transformed mouse embryonic fibroblast (MEF) model, we demonstrated that TRAF2 binding  
80 was required for cIAP1 pro-tumoral activity. cIAP1 induced the clustering of TRAF2, which was sufficient to engage  
81 pro-tumoral signaling pathways independently of receptor engagement. A novel function for cIAP1 is therefore  
82 identified that appears essential for TRAF2 to associate with its protein partners. As expected, cIAP1/TRAF2 complex  
83 promoted the activation of the canonical NF- $\kappa$ B signaling pathway. Among mitogen-activated protein kinase (MAPK)  
84 signaling pathways, it stimulated ERK1/2 whereas it inhibited p38 and did not affect JNK pathway. cIAP1/TRAF2  
85 promotes NF- $\kappa$ B dependent production of IL-6 that activates JAK2/STAT3 signaling pathway in an autocrine manner.  
86 Finally, we demonstrated for the first time that STAT3 activation was critical for the tumor-promoting activity of  
87 cIAP1/TRAF2.

## 90 **Results**

### 92 **1. Binding to TRAF2 is critical for the oncogenic activity of cIAP1.**

93 We generated a cIAP1-deficient tumor model by transforming immortalized wt, *clap1*<sup>-/-</sup> (SKO) or *clap1*<sup>-/-</sup>/*clap2*<sup>-/-</sup>  
94 (DKO) mouse embryonic fibroblasts (MEFs) (from J. Silke & D. Vaux's laboratories) by the HRas-V12 oncogene (Fig.  
95 1A). Deletion of cIAP1 slowed down tumor growth in a xenograft model (Fig. 1B) and decreased the formation of lung  
96 cancer foci when the cells were injected into the tail vein (Fig. 1C). Double deletion of cIAP1 and cIAP2 amplified the  
97 phenomena (Fig. 1B and 1C). Rescue experiments demonstrated that restoring cIAP1 in single-knockout (SKO) or  
98 double-knockout (DKO) cells (Fig. 1D) significantly enhanced tumor cell growth (Fig 1B & 1E) confirming the oncogenic  
99 properties of cIAP1. We next stably expressed cIAP1 mutants unable to bind TRAF2 in Hras-V12-transformed DKO-MEFs  
100 (Fig. 1F). The mutants previously validated (11) are cIAP1 <sup>$\Delta$ BIR1</sup> in which the BIR1 has been deleted, and cIAP1<sup>L47A</sup> mutant  
101 in which a point mutation within the BIR1 has been introduced. We checked that these mutants lost their ability to  
102 bind TRAF2 (Fig S1A) and conserved their full E3-ligase activity by treating the cells with the smac mimetic GDC-0152,  
103 known to stimulate the self-ubiquitination and degradation of cIAP1 (Fig S1B). Deletion of the BIR1 as well as mutation  
104 of Leucine 47 were sufficient to completely abolish the oncogenic activity of cIAP1, as demonstrated both in our  
105 xenograft model (Fig 1G) and in the experimental metastasis model (Fig 1H). Re-expression of cIAP1 into DKO also  
106 increased the number of the colonies formed in soft agar medium and deletion of BIR1 abolished the capacity of cIAP1

107 to stimulate anchorage-independent cell growth (Fig 1I). By comparison, deletion of BIR2 ( $\Delta$ BIR2) did not significantly  
108 alter the clonogenic properties (Fig 1I) of cIAP1. Of note, the mutant  $\Delta$ BIR1, devoid of oncogenic properties, was  
109 strongly expressed compared to the native full length cIAP1 (Fig 1F, S1B). These results demonstrate that TRAF2  
110 binding is required for cIAP1 to stimulate tumor growth. It is worth noting that we were unable to obtain TRAF2  
111 depleted MEFs (either by guide-RNA genome editing or shRNA), suggesting that the deletion of TRAF2 caused cell  
112 death as already reported (15).

## 114 **2. Clustering of TRAF2 is sufficient to stimulate tumor growth**

115 An immunofluorescence analysis demonstrated the presence of cytoplasmic TRAF2 clusters in DKO-cIAP1 but  
116 not in DKO-cIAP1 <sup>$\Delta$ BIR1</sup> (Fig 2A). Whereas these clusters did not colocalize with markers of calveola (calveolin-1), golgi  
117 apparatus (GM130) or lysosomes (LAMP-1), they colocalized with the endoplasmic reticulum marker PDI (Fig 2B).  
118 Structural analyzes demonstrated that the BIR1 of cIAPs can bind a TRAF1/2 trimer (16, 17). We hypothesized that  
119 cIAP1 could trigger the oligomerization of TRAF2 required for partner binding and the activation of downstream  
120 signaling pathways (18). We forced the trimerization of TRAF2 by expressing isolated BIR1 (iBIR1) in DKO-MEFs using  
121 a retroviral infection (Fig 2C). As expected, we observed the clustering of TRAF2 in iBIR1-expressing cells (Fig 2A). The  
122 expression of iBIR1 increased the clonogenic growth of cells, forming large and dense colonies (Fig 2D) and was as  
123 efficient as cIAP1 to stimulate the tumor growth in mice (Fig 2E). Expression of iBIR1 in wt MEFs also stimulated tumor  
124 growth (Fig S2A), although the presence of iBIR1 strongly sensitized cells to TNF $\alpha$ -induced cell death (Fig S2B) as a  
125 result of a competitive inhibition of cIAP1-TRAF2 association (Fig S2C). These results suggest that TRAF2 clustering is  
126 sufficient to engage pro-tumoral signaling pathways, independently of TNFR stimulation.

## 128 **3. cIAP1 is critical for TRAF2 interactome.**

129 We then investigated the influence of cIAP1 on TRAF2 protein-interacting network. The TRAF2 interactome was  
130 analyzed in cell treated with the smac mimetics GDC0152 that completely depleted cIAP1 whereas it weakly enhanced  
131 cIAP2 and XIAP and did not affect TRAF2 protein levels (Fig 3A). TRAF2 partners were identified by performing  
132 immunoprecipitation (Fig S3A) followed by mass spectrometry analysis (Table S1). The data were analyzed using the  
133 functional enrichment analysis tool (FunRich) and the UniProt database. We detected 419 to 797 hits in the untreated  
134 cells (Fig 3B). As expected, we found TRAF1 and cIAP1 (BIRC2), which was the only IAP detected in the screen (Fig 3C).

135 In accordance with its role as a signaling adaptor, we observed an enrichment of TRAF2 partners in the membrane,  
136 protein-containing complex and membrane raft compartments (Fig 3D). However, TRAF2 partners were also enriched  
137 in the cytoplasm, cytosol and nucleus (Fig 3D, S3B). Concerning biological processes, as expected, TRAF2 partners  
138 were enriched among proteins involved in TNF-mediated, NF- $\kappa$ B and MAPK-signaling pathways, apoptosis regulation,  
139 proteins ubiquitination and regulation of protein turn-over (protein stabilization and ubiquitin/proteasome system)  
140 (Fig 3E, S4). Interestingly, TRAF2 partners were also significantly enriched among proteins involved in epithelial cell  
141 differentiation-related pathways (Fig 3E, S4). Use of the FunRich database confirmed a strong enrichment of TRAF2  
142 partners in the ErbB-mediated signaling network, compared to that observed in the TNFR-signaling pathway (Fig S5).  
143 Moreover, TRAF2 partners were enriched in cdc42-associated signaling pathways but not in RhoA or Rac1-related  
144 signaling events (Fig 3C, S5), which is consistent with our previous work showing that the cytoplasmic cIAP1/TRAF2  
145 complex controls the activation cycle of cdc42 RhoGTPase in unstimulated fibroblasts (11).

146 cIAP1 depletion drastically decreased (about 70%) the number of hits (Fig 3B, 3F). However, it did not affect  
147 the binding of TRAF2 to TRAF1 (Fig 3C) and it did not significantly modify the distribution of TRAF2 partners in the  
148 different subcellular compartments, biological processes or signaling pathways (Fig 3D, 3E, S3B, S4, S5). Nevertheless,  
149 we observed a trend towards increased TRAF2 partners in negative regulation of apoptosis and protein stabilization  
150 pathways (Fig 3E & S4). Thus, cIAP1 appears critical for the binding of TRAF2 to its protein partners.

151

#### 152 **4. cIAP1/TRAF2 induces the activation of NF- $\kappa$ B and ERK1/2 signaling pathways in H-Ras-V12 transformed** 153 **MEFs.**

154 We analyzed the signaling pathways activated in HRas-V12-transformed MEFs. As expected, cIAP1-expressing  
155 MEFs displays a downregulation of I $\kappa$ B- $\alpha$  (Fig 4A) that characterizes the activation of the canonical NF- $\kappa$ B signaling  
156 pathway. This marker was not observed in the mutant cIAP1-expressing cells (Fig 4A). Accordingly, an RT-PCR array  
157 showed a general upregulation of NF- $\kappa$ B-target genes in wt cIAP1-expressing MEFs compared to cIAP1 <sup>$\Delta$ BIR1</sup>-expressing  
158 cells (Fig 4B). On the other hand, the p52 NF- $\kappa$ B active-subunit that is mainly expressed in the nuclei-enriched fraction  
159 in DKO cells was found in the cytoplasm in cIAP1-expressing MEFs and even more in cIAP1 <sup>$\Delta$ BIR1</sup>-expressing MEFs  
160 demonstrating that cIAP1 or its mutant inhibited the non-canonical NF- $\kappa$ B activating pathway (Fig 4C). Among MAPK  
161 signaling pathways, expression of cIAP1 but not cIAP1 mutants simulated ERK signaling characterized by ERK1/2  
162 phosphorylation, decreased phosphorylation of p38 and did not affect the c-Jun N-terminal kinase (JNK) signaling

163 pathway (Fig 4A). Of note, the expression of cIAP1 or its  $\Delta$ BIR1 mutant did not significantly modify the expression level  
164 of TRAF2 and RIP1 (Fig 4A).

### 165

166 **5. cIAP1/TRAF2 promotes NF- $\kappa$ B-dependent production of IL-6 leading to an activation of JAK/STAT3**  
167 **signaling pathway in an autocrine manner.**

168 We observed the activation of JAK2 and STAT3 characterized by their phosphorylation at Y1008 and Y705  
169 residue respectively in cIAP1-expressing MEFs but not in cells expressing cIAP1 mutants (Fig 5A & B). Silencing of TRAF2  
170 decreased cIAP1-mediated STAT3 phosphorylation, confirming the importance of TRAF2 in this process (Fig 5C). We  
171 then analyzed the contribution of NF- $\kappa$ B and ERK signaling pathway in STAT3 activation. Inhibition of the NF- $\kappa$ B  
172 signaling pathway by Bay-11-7082 prevented STAT3 phosphorylation while inhibition of the MEK/ERK axis by  
173 trametinib did not modify it (Fig 5D), demonstrating a NF- $\kappa$ B-dependent activation of STAT3 pathway. Conversely, the  
174 STAT3 inhibitor niclosamide did not modify ERK and weakly decreased I $\kappa$ B- $\alpha$  phosphorylation (Fig 5D). Trametinib did  
175 not interfere with I $\kappa$ B- $\alpha$  phosphorylation and Bay-11-7082 did not modify ERK phosphorylation (Fig 5D), showing that  
176 the 2 pathways were activated independently. JAK2/STAT3 signaling axis can be activated by stimulation of cytokine-  
177 or growth factor receptors such as IL-6R or EGFR. Consistent with the activation of NF- $\kappa$ B, cIAP1 expression induced  
178 upregulation of the NF- $\kappa$ B target gene *IL-6* which is inhibited by the NF- $\kappa$ B inhibitor Bay-11-7082 but not by the MEK  
179 inhibitor Trametinib (Fig 5E). In contrast, the expression of cIAP1 <sup>$\Delta$ BIR1</sup> was not able to stimulate *IL-6* expression (Fig 5E).  
180 Inhibition of IL-6 by an anti-IL-6 neutralizing antibody completely blocked STAT3 phosphorylation in cIAP1-restored  
181 MEFs (Fig 5F). Altogether, these results demonstrated that the expression of cIAP1 stimulated the NF- $\kappa$ B-dependent  
182 production of IL-6 that induced an autocrine activation of the JAK2/STAT3 signaling pathway. By analyzing available  
183 cancer genome atlas (TCGA) dataset of the national cancer institute (NIH) using the gene expression profiling  
184 interactive analysis software (GEPIA)(19), we observed a significant correlation between the cIAP1-encoding *BIRC2*  
185 and *IL6* gene expression in lung adenocarcinoma (LUAD), breast invasive carcinoma (BRCA) and thyroid carcinoma (THCA)  
186 (Fig 5G). In contrast, no correlation between *TNF* and *BIRC2* expression was detected (Fig S6). We then investigated  
187 the role of cIAP1 and TRAF2 in JAK/STAT3 signaling in the lung adenocarcinoma cell line A549 (Fig 5H & I). Silencing of  
188 cIAP1 or TRAF2 inhibited basal JAK2 and STAT3 phosphorylation (Fig 5H). Similarly, depletion of cIAP1 by GDC-0152  
189 inhibited JAK2 and STAT3 phosphorylation in a dose-dependent manner (Fig 5I).

## The JAK/STAT3 signaling pathway is involved in cIAP1-mediated tumor growth.

We then evaluated the contribution of STAT3 and MEK/ERK signaling pathways in cIAP1/TRAF2 mediated-tumor growth using the STAT3 inhibitor niclosamide and the MEK inhibitor trametinib. Niclosamide or trametinib were daily injected intraperitoneally when the tumors reached a volume of approximately 100 mm<sup>3</sup>. Niclosamide treatment selectively slowed down the growth of DKO-cIAP1 MEFs in mice, neutralizing the growth advantage given by cIAP1 expression, whereas it did not modify the growth of cIAP1<sup>ΔBIR1</sup> expressing MEFs (Fig 6A & B). In contrast, trametinib inhibited the growth of both MEFs expressing cIAP1 and the ΔBIR1 mutant (Fig 6C & D), which is consistent with the role of MEK/ERK signaling pathway in the transforming activity of HRas-V12. We then confirmed the importance of STAT3 in the growth/survival of cIAP1-expressing MEFs in a clonogenic and crystal violet assay (Fig 6E-G). Inhibition of STAT3 by niclosamide abolished the clonogenic advantage of cIAP1-reconstituted MEFs (Fig 6E) and siRNA-mediated-silencing of STAT3 did not affect the survival of DKO but selectively decreased cIAP1-expressing DKO MEFs count (Fig 6G).

### Discussion:

TRAF2 serves as an adaptor protein to bring the cIAP1 E3-ubiquitine ligase closer to its substrates. It can also stabilize cIAP1 protein by blocking its autoubiquitination and degradation (20) and, in some situations, it can activate its E3-ubiquitine ligase activity through K63-linked ubiquitination (21). Conversely, cIAP1 can regulate TRAF2 stability by controlling its ubiquitin-proteasome system (UPS)-mediated degradation (14, 22, 23). In the present work, we extend our understanding of cIAP1's hold over TRAF2 by showing that cIAP1 is critical for TRAF2 binding to its protein partners.

The function of TRAF2 as a molecular adaptor allowing the recruitment of signaling molecules into receptor-associated signaling complexes has been well reported. However, there is converging evidences pointing at the existence of a cIAP1-TRAF2 complex in the cytoplasm and nucleus of unstimulated cells. Shu *et al.* demonstrated in 1996 that cIAP1-TRAF2 binding occurs in the cytoplasm and that they are recruited together to TNFR1-associated complex in TNFα-stimulated cells (24). The TRAF2 protein has a mushroom-like shape. The cap is formed by the C-terminal half of the conserved TRAF domain (called TRAF-C) that mediates binding to receptors, and the stem is formed

218 by the coiled-coiled N-terminal half of the TRAF domain (TRAF-N), the zing fingers and a N-terminal RING domain  
219 required for downstream signaling (18, 25). Whereas the mechanisms of interaction of TRAF2 with receptors have  
220 been the subject of numerous studies, the binding of TRAF2 with signaling molecules is much less clear. The trimeric  
221 form of TRAF2 binds to activated trimeric receptor (26-28). By contrast, a TRAF2 trimer interacts with only one cIAP1  
222 molecule (16, 17). The oligomerization of the amino-terminal half of TRAF2 is also necessary for the recruitment of  
223 downstream signaling effectors (18). The oligomerization site is located in the coiled-coiled TRAF-N domain (26). Of  
224 interest, cIAP1 binds a motif called CIM (cIAP1/2-interacting motif) found at the N-terminal extremity of the TRAF-N  
225 (16). We may hypothesize that cIAP1 primes TRAF2 for its binding to partners, whether receptors or signaling effectors,  
226 by maintaining it in a proficient oligomerized form. Accordingly, we show here that a forced oligomerization of TRAF2  
227 induced by expressing the cIAP1-BIR1 domain is sufficient to engage tumor promoting signaling pathways. Our  
228 proteomic analysis revealed that, in the presence of cIAP1, TRAF2 could bind proteins found in different subcellular  
229 compartments and involved in different cellular processes. The large number of partners found in the screen suggest  
230 that many proteins could potentially be substrates of the cIAP1-TRAF2 E3-ubiquitine ligase complex. Among the TRAFs,  
231 we found TRAF1, which is known to bind TRAF2 to form a TRAF1:(TRAF2)<sub>2</sub> heterotrimer displaying a higher affinity for  
232 cIAP2-BIR1 than the TRAF2 homotrimer (17). Interestingly, depletion of cIAP1 did not affect TRAF2-TRAF1 interaction.  
233 Since the analysis has been performed in unstimulated cells, we did not detect receptors in the screen. As expected,  
234 TRAF2 partners included proteins involved in TNFR-mediated signaling pathways such as NF-κB, MAPK or apoptosis  
235 regulation. In accordance with the E3-ubiquitine ligase activity of the cIAP1/TRAF2 complex, we also found an  
236 enrichment of TRAF2 partners involved in ubiquitination-related processes. Interestingly, we observed a strong  
237 enrichment of TRAF2 partners among proteins of signaling networks of the ErbB receptors which are activators of the  
238 STAT3 axis. Although an interaction of TRAF2 with ErbB receptors has never been observed, a role for TRAF2 in EGF-  
239 mediated tumor growth has been reported (29).

240  
241 We demonstrated that TRAF2 is required for the oncogenic activities of cIAP1 in HRas-V12 expressing cells. The  
242 expression of cIAP1 appeared altered in a number of human tumor samples and its overexpression has been correlated  
243 with advanced progressive disease, aggressiveness and poor prognosis or low response to treatment (for review, see  
244 (30)). Its oncogenic properties have been clearly demonstrated in murine models. In 2006, Zender *et al.* demonstrated  
245 that the overexpression of cIAP1 facilitated the growth of p53<sup>-/-</sup>, c-myc-expressing hepatocarcinoma cells in

246 immunodeficient recipient mice. Inversely downregulation of cIAPs in hepatocarcinoma cells that display a recurrent  
247 amplification at the chromosome region containing cIAP1, cIAP2 and Yap1-encoding genes (9qA1 amplicon) selectively  
248 slowed down tumor growth (5). Similarly, Ma *et al.* showed that the down-regulation of cIAP1 or cIAP2 selectively  
249 affected the growth rate of 9A1 amplicon-harboring, p53<sup>-/-</sup> osteosarcoma transplanted into nude mice (6). In 2010,  
250 Cheng *et al.* demonstrated a high level of expression of cIAP1 and cIAP2 in mammary carcinoma and that the silencing  
251 of cIAP1 and/or cIAP2 resulted in decreased tumor growth in an orthotopic breast transplantation model (7). The  
252 molecular mechanisms driving these oncogenic activities have not been clearly determined and they probably depend  
253 on the oncogenic contexts. The various signaling pathways controlled by cIAPs may account for their tumorigenic  
254 functions. The ability of cIAP1 to regulate NF-κBs, a major pro-survival, oncogenic signaling pathway is undeniably of  
255 importance in its transforming potential (13, 31, 32). The c-myc repressor Mad1 is an ubiquitination target of cIAP1(33,  
256 34). Thus, the oncogenesis-promoting activity of c-myc can be amplified by cIAP1-mediated downregulation of Mad1.  
257 In the present work, we highlighted the importance of the interaction cIAP1 with its protein partner TRAF2 in HRas-  
258 V12-driven tumorigenesis. Indeed, preventing the interaction with TRAF2 by deletion or mutation of the BIR1 domain  
259 completely abolished the oncogenic potential of cIAP1.

260 The role of cIAP1-TRAF2 in regulating signaling pathways has been extensively analyzed in the context of stimulation  
261 of receptors from the TNFR, IL-R or PRR families (recently reviewed in a special issue of *Frontiers in Immunology* (35)).  
262 Although we cannot rule out that some membrane receptors could be activated by tumor- or host-produced soluble  
263 factors in an autocrine or paracrine manner, the oligomerization of TRAF2 by cIAP1 or isolated cIAP1-BIR1 seems  
264 sufficient to stimulate tumor-promoting signaling pathways, independently of the stimulation of receptors.  
265 Accordingly, Baud *et al.* demonstrated that the overexpression of TRAF2 or oligomerization of its amino-terminal  
266 domains was sufficient to activate downstream signaling pathways (18). TRAF2 can directly bind, via its N-terminal half  
267 that includes the zing fingers and a N-terminal RING domain, several MAP3Ks including the mixed-lineage protein  
268 kinase 3 (MLK3) (36, 37) and ASK1 (38, 39) that drive the activation of SAPK/JNK and p38-MAPK axes, and MEKK1 that  
269 induces the activation of downstream SAPK/JNK and NF-κB (18, 40). The ubiquitin chains conjugated by the  
270 cIAP1/TRAF2 E3-ubiquitin ligase complex (to RIP1 or via a self-ubiquitination process) are scaffolds for the recruitment  
271 of TAK1 and IKKγ that lead to MAPK and canonical NF-κB activation (41). Moreover, cIAP1 can control the activation  
272 of the RAF-MEK-ERK1/2 cascade by ubiquitinating cRAF (42). In the present work, we observed that the tumor-  
273 promoting activity of cIAP1/TRAF2 was associated with an activation of the canonical NF-κB and ERK1/2 whereas JNK

274 and p38MAPK signaling pathways were unaffected or inhibited. More investigations will be required to determine the  
275 downstream effectors. Expressing cIAP1 induced a decreased in the non-canonical activation of NF- $\kappa$ B, in accordance  
276 with its capacity to target NIK to UPS-mediated degradation (21, 43). The deletion of the BIR1 domain amplified the  
277 phenomena. Lee *et al.* identified an IBM (IAP-binding motif) at the N-terminus of NIK protein sequence (43). The NIK-  
278 IBM is recognized by the BIR2 domain of cIAP1 and constitutes a substrate recognition signal for cIAP1-mediated  
279 ubiquitination and degradation (43). We may hypothesize that the deletion of BIR1 could improve the accessibility to  
280 the BIR2 domain leading to an enhanced recruitment and degradation of NIK.

281 Last, we demonstrate here that cIAP1/TRAF2 promotes the activation of the JAK/STAT3 axis. The activation of this  
282 signaling pathway results from an NF- $\kappa$ B-dependent production of IL-6 and autocrine activation of IL-6 signaling  
283 pathway. The presence of IL-6 in the tumor environment and hyperactivation of the JAK/STAT3 signaling pathway in  
284 cancer cells have been found in different kind of tumors (44). The analysis of TCGA dataset revealed a positive  
285 correlation between cIAP1-encoding gene and *IL-6* in lung, breast and thyroid carcinoma. The smac mimetic GDC-0152  
286 as well as downregulation of cIAP1 or TRAF2 were able to decrease the activation of STAT3 in A549 lung carcinoma  
287 cells suggesting that cIAP1/TRAF2 could account for the activation of STAT3 in these cells. Interestingly, we show here  
288 that inhibition of STAT3 by niclosamide completely abrogated the tumor growth advantage given by expressing cIAP1  
289 demonstrating that the activation of the STAT3 axis is required for the tumor-promoting activity of cIAP1.

290  
291 The current model supports that TRAF2 acts solely as an adaptor protein recruiting the cIAP1/cIAP2 E3-ligase  
292 in the receptor-associated complex. Our work demonstrates that (i) oligomerisation of TRAF2 is sufficient to stimulate  
293 pro-tumoral signaling pathways, (ii) TRAF2 is a critical regulator of the oncogenic activity of cIAP1 and (iii) cIAP1 is  
294 essential for TRAF2' capacity to bind signaling molecules, independently of receptor activation. The cIAP1-encoding  
295 *BIRC2* gene as well as *TRAF2* are found recurrently amplified in human epithelial cancers (30, 45). IAPs constitute  
296 promising target for anticancer therapy and a number of IAP antagonists have been developed and are currently under  
297 clinical investigation (30). Most of them are Smac mimetics that block the anti-apoptotic activity of XIAP and induce  
298 the degradation of cIAP1 and, in some cases, other members of the IAP family. Considering our results, it could be  
299 interesting to develop molecules able to inhibit the oligomerisation of TRAF2 or the cIAP1-TRAF2 interaction.

301 **Materials and methods:**

302 Cell culture and treatments:

303 SV40 immortalized wt, cIAP1<sup>-/-</sup> (single Knock out, SKO) and cIAP1<sup>-/-</sup>/cIAP2<sup>-/-</sup> (double KO, DKO) mouse embryonic  
304 fibroblasts (MEFs) (J. Silke & D. Vaux, Melbourne, Australia), A549 human lung carcinoma cell line, HeLa cervical  
305 carcinoma cell line and Phoenix-Eco 293T cells (Invitrogen, Carlsbad, USA) were cultured in DMEM (Dulbecco's  
306 modified Eagle's medium, Dominique Dutscher, Brumath, France) high glucose medium supplemented with 10% fetal  
307 bovine serum (Dominique Dutscher) at 37°C, 5% CO<sub>2</sub> environment. MEFs were transformed by HRas-V12 as previously  
308 described (11). MEFs were treated with 1-2μM niclosamide, 2μM Bay-11-7082, 2μM Trametinib (Euromedex,  
309 Souffelweyersheim, France) or 100 ng/mL anti-IL-6 neutralizing antibody (Invivogen, San Diego, USA). GDC0152  
310 (Euromedex) was used at 1 to 5μM.

311

312 Plasmid constructs, siRNAs, cell transfection and viral transduction:

313 Plasmids used were: pMSCV-control, pMSCV-cIAP1, pMSCV-cIAP1ΔBIR1, pMSCV-cIAP1ΔBIR2, pMSCV-cIAP1-L47A,  
314 pMSCV-iBIR1 (cIAP1). Cells were transfected using Jet PEI transfection reagent (Polyplus transfection, Ozyme, France)  
315 for plasmids or Lipofectamine<sup>®</sup> RNAimax (Thermofisher Scientific, Waltham, USA) for siRNAs against human cIAP1  
316 (#SI02654442), human TRAF2 (#SI00129619), mouse TRAF2 (#SI01454544) or human STAT3 (#1: SI01435294 and #2:  
317 SI01435287) from Qiagen (Hilden, Germany). Phoenix-Eco 293T cells used for viral production were transfected using  
318 Jet PEI. For the infection of MEFs, retrovirus-containing supernatant was supplemented with 1μg/mL of polybrene  
319 (Sigma-Aldrich, St-Louis, USA). Cells were selected with 2.8μg/mL of puromycine.

320

321 In vivo experiments:

322 Nude (NMRI-Foxn1nu/Foxn1nu) mice (Charles River Laboratories, Saint-Germain-Nuelles, France) (female between 6  
323 and 8 weeks old) were housed in pathogen free conditions in zootechny center (certification n°C21 464 04 EA). All  
324 studies were approved by the Ethics Committee for Animal Welfare of the University of Burgundy and the French  
325 Ministry of Higher Education and Research (APAFIS#5438-201611301622214). For subcutaneous tumors, mice were

326 randomized and inoculated subcutaneously with 500 000 or 750 000 HRas-V12-transformed MEFs. When the tumors  
327 reached 100mm<sup>3</sup>, mice were allocated into experimental groups so that the mean +/- SD was equivalent in each of the  
328 groups and daily treated intraperitoneally with niclosamide (30 mg/Kg), trametinib (1mg/kg) or vehicle. Tumor volume  
329 was measured with calipers and calculated as proposed by Laval University (Québec, Canada):  
330  $(4/3)*3.14159*(length/2)*(width/2)^2$ . For artificial metastasis model, HRas-V12-transformed MEFs were injected into  
331 the tail vein (10<sup>6</sup>) in a volume of 100µL. Mice were sacrificed 36 days after intravenous injection of the cells. Lung  
332 nodes were counted by macroscopic analysis. The experiments were performed at least twice n=6-10 per group.  
333 Statistical analyses were performed using the Mann Whitney test.

334

#### 335 Cell extracts, subcellular fractionation, immunoprecipitation and Western Blot:

336 Cells were washed in cold 1X DPBS (Dulbecco's Phosphate Buffer Saline, Dominique Dustcher, Brumath, France) and  
337 lysed in RIPA buffer (50mM Tris-HCl pH 8,0 ; 150mM NaCl ; 1% NP-40 ; 0.5% Sodium deoxycholate, 0.1% SDS, 1mM  
338 sodium orthovanadate, 1mM PMSF) supplemented with a proteases inhibitor cocktail (PIC, Sigma-Aldrich, St-Louis,  
339 USA) and phosphatase inhibitor cocktail PhosSTOP™ (Merck, Darmstadt, Germany). The subcellular fractionation was  
340 performed by lysing cells in 10mM Hepes, 10mM KCl, 0.1mM EDTA, 0.1mM EGTA, 1mM DTT (DiThioThreitol) for 15  
341 minutes on ice. NP-40 (0.6% final) was added to the lysate which then subjected to centrifugation at 1200g for 5  
342 minutes at 4°C. The supernatant containing the cytoplasmic fraction was collected. The pellet was lysed in 100µL of  
343 50mM Tris-HCL pH8.0, 150mM NaCl, 1%NP-40 for 15 minutes on ice. The solution was centrifuged at 16000g for 15  
344 minutes at 4°C and the supernatant containing the nuclear fraction is collected. Proteins were quantified using the  
345 Precision Red Advanced Protein Assay ADV02 kit (Cytoskeleton, Denver, USA).

346 For Immunoprecipitation, cells were lysed in IP buffer (50mM Tris HCL pH7.4, 150mM NaCl, 20mM EDTA, 0.5% NP-  
347 40, Protease inhibitor cocktail 1X). Cell lysates were incubated with anti-TRAF2 (#ab126758, Abcam, Cambridge, UK)  
348 antibodies overnight at 4°C. The lysates were then incubated 2 hours with G Sepharose beads (Merk-Millipore,  
349 Fontenay-sous-bois, France). Proteins were eluted by heating the mix to 95°C for 10 minutes in 1X Laemmli buffer  
350 (Tris-HCl 150 mM pH 6,8 ; β-mercaptoethanol 15 %; SDS 6 %; glycerol 30 %; Bromophenol blue). For the Western blot  
351 analysis, proteins were separated on SDS-PAGE and electro-transferred onto polyvinylidene difluoride or nitrocellulose

352 membranes (GE Healthcare, Dominique Dutscher, Brumath, France). Blots were probed with the following antibodies:  
353 anti-clAP1 (#AF8181, R&D systems, Minneapolis, USA) and anti-pan-clAPs (#MAB3400, R&D systems, Minneapolis,  
354 USA), anti-TRAF2 (#ADI-AAP-422, Enzo Life Sciences, Villeurbanne, France), anti-RIP1 (#610459, BD biosciences, USA),  
355 anti-I $\kappa$ B $\alpha$  (#4812S), anti-p-I $\kappa$ B $\alpha$  (S32, #2859S), anti-ERK1/2 (#4695T), anti-p-ERK1/2 (Y202/204, #4370T), anti-JNK  
356 (#9252T), anti-p-JNK (T183/Y185, #81E11), anti-p38 (#D13E1), anti-p-p38 (T180/Y182, #D3F9), anti-STAT3 (#D3Z2G),  
357 anti-p-STAT3 (Y705, #D3A7), anti-JAK2 (#D2E12) and anti-p-JAK2 (Y1008, #D4A8) and anti-p100/p52 NF $\kappa$ B (#4882)  
358 from Cell signaling technologies (Danvers, USA), anti-HSC70 (sc-7298, Santa Cruz Biotechnology Inc, Dallas, USA) and  
359 anti- $\beta$ -actin (#MA1-140 Invitrogen, Waltham, USA), Anti-XIAP (AF8221, R&D systems) and anti-Ras (sc-520, Santa cruz  
360 Technology Inc). Detection was performed using peroxidase-conjugated secondary antibodies and chemiluminescence  
361 detection kit (Clarity<sup>TM</sup> or Clarity Max<sup>TM</sup> western ECL substrate, Bio-Rad, Marnes-la-Coquette, France). GST-pull down  
362 assays were performed as previously described (11).

363

364 Immunofluorescence: Cells were washed in cold 1X DPBS and fixed for 10 min in 4% paraformaldehyde/PBS,  
365 permeabilized using 0.1% triton X-100 (10 minutes) and saturated for 20 minutes in PBS with 1% bovine serum albumin  
366 and 1% of fetal bovine serum. Samples were incubated overnight at 4°C in PBS-1%BSA with primary antibodies anti-  
367 GM130 (#610823, BD Bioscience), anti-Caveolin-1 (#MA3-600, Invitrogen), anti-LAMP-1 (#ab25245, Abcam) or anti-  
368 PDI (#3501, Cell Signaling), washed and incubated with secondary antibodies goat anti-rat Alexa568, goat anti-mouse  
369 alexa568 or donkey anti-rabbit Alesa568 (Invitrogen) diluted in PBS-1%BSA at room temperature for 1h. Samples were  
370 then incubated with Alexa488 labeled anti-TRAF2 antibody (Abcam ab198971) diluted in PBS-1%BSA overnight at 4°C.  
371 Samples were washed for 10 minutes three times, then mounted using ProLong<sup>TM</sup> Gold Antifade Mountant with DAPI  
372 (Thermofisher Scientific, Waltham, USA). Sample images were acquired using an Axio Imager 2 using an Apotome.2  
373 module, HXP 120C illumination, AxioCam MRm using a 64x 1.4NA objective.

374

375 RNA extraction and RT-qPCR: Total RNA of MEF DKO expressing or not clAP1 or its mutants were extracted with Trizol  
376 reagent (TRizol Reagent<sup>®</sup>, Invitrogen) according to manufacturer's protocol. Tumors from in vivo experiments were  
377 crushed in 1mL of Trizol to extract their RNA. cDNA was produced from 1 $\mu$ g of RNA with iScript cDNA synthesis kit

378 (Biorad, Hercules, USA). Quantitative real-time PCR was performed with ViiA 7 Real-Time PCR System (Applied  
379 Biosystem, ThermoFisher Scientific, Waltham, USA) using Master Mix Applied Biosystems™ PowerUp™ SYBR™ Green  
380 (Thermofisher Scientific, Waltham, USA) and the following primers:  $\beta$ -Actin Forward : CGG-TTC-CGAT-GCC-CTG-AGG-  
381 CTC-TT, Reverse : CGT-CAC-ACTTCA-TGA-TGG-AAT-TGA ; IL-6 (Interleukine 6) Forward : TGA-TGC-ACT-TGC-AGA-AAA-  
382 CA, Reverse : ACC-AGA-GGA-AAT-TTT-CAA-TAG-GC.

383 For the qPCR microarray, cDNA from MEF DKO-clAP1 and MEF DKO-clAP1 $\Delta$ BIR1 RNA were analyzed using Qiagen NF-  
384  $\kappa$ B Signaling Pathway RT<sup>2</sup> Profiler PCR Array according to manufacturer's protocol.

385 Clonogenic assay: Five thousand MEFs were seeded in soft-agar medium for 3 weeks at 37°C in a 5% CO<sub>2</sub> atmosphere.  
386 They were treated with 1-2  $\mu$ M Niclosamide before plating. Colony number and size were analyzed under microscope  
387 (Zeiss, Oberkochen, Germany), and images were taken using AxioVision software.

388 Cristal violet assay: One hundred thousand were plated in 6-wells plate. Seventy-two hours later, cells were fixed and  
389 stained with a 0.5% Crystal violet in methanol solution. Crystal violet was eluted with 37% acetic acid, and the OD at  
390 620nm was measured with a UVM 340 plate reader (Biochrom, Cambourne, UK).

391 Mass-spectrometry: A549 cells were treated or not with 5 $\mu$ M of GDC-0152 for 6 hours. TRAF2 was immunoprecipitated  
392 and eluted. ESI-TRAP mass spectrometry was performed by the CLIPP platform as described previously (46) Data were  
393 analyzed with FunRich software, version 3.1.3 (Functional enrichment analysis tool)(47), using the human Uniprot or  
394 FunRich database.

395

396 Statistical analysis: the correlation analysis of the clAP1, IL-6 and TNF- $\alpha$  expression in tumor samples was done using  
397 the publicly available TCGA dataset using gene expression profiling interactive analysis (GEPIA), using the Pearson  
398 Correlation Coefficient. The non-parametric Mann–Whitney test was used for the analysis of tumor growth in animals  
399 and RT-qPCR and Wilcoxon test for clonogenic and western blot analyses.

400

401 **Acknowledgements.** We thank Pauline Maes from the CLIPP proteomic platform, University of Burgundy, Philippe  
402 Hammann from the Strasbourg proteomic platform, IBMC, Valérie Saint-Gorgio from zootechny center, University of  
403 Burgundy and Romain Aucagne from the Crigen platform, University of Burgundy. This work was supported by grants

404 from the 'Comités de Côte d'Or et de l'Yonne' of the 'Ligue Contre le Cancer' (LD), La Ligue Nationale contre le Cancer  
405 (CG's team), the European Union and the 'Conseil Régional de Bourgogne', a French Government grant managed by  
406 the French National Research Agency under the program 'Investissements d'Avenir' with reference ANR-11-LABX-  
407 0021, and fellowships from the 'Ministère de l'Enseignement Supérieur et de la Recherche' of France (to BD, AZ, JB  
408 and JA), the 'Fondation ARC pour la Recherche sur le Cancer' (to BD). We thank the FEDER for their financial support.

409  
410 **Author contributions.** BD and AZ performed most of the experiments and analyzed the data. JB initiated the project,  
411 established the tumor model and performed some *in vivo* experiments. SC performed immunofluorescence analysis.  
412 JA, PB and FC helped in performing western blots, clonogenicity assays and *in vivo* experiments. CR and CP brought  
413 expertise in *in vivo* model and performed IV injection. CG provided scientific expertise and corrected the paper and LD  
414 conceived and supervised the project, conducted the GEPIA analysis, analyzed the data and interpreted the results,  
415 wrote the paper with input from all authors.

## 416 417 418 **References**

- 419  
420 1. Rothe M, Pan MG, Henzel WJ, Ayres TM, Goeddel DV. The TNFR2-TRAF signaling complex contains two novel  
421 proteins related to baculoviral inhibitor of apoptosis proteins. *Cell*. 1995;83(7):1243-52.  
422 2. Hrdinka M, Yabal M. Inhibitor of apoptosis proteins in human health and disease. *Genes Immun*.  
423 2019;20(8):641-50.  
424 3. Dumetier B, Zadoroznyj A, Dubrez L. IAP-Mediated Protein Ubiquitination in Regulating Cell Signaling. *Cells*.  
425 2020;9(5).  
426 4. Zadoroznyj A, Dubrez L. Cytoplasmic and Nuclear Functions of cIAP1. *Biomolecules*. 2022;12(2).  
427 5. Zender L, Spector MS, Xue W, Flemming P, Cordon-Cardo C, Silke J, et al. Identification and validation of  
428 oncogenes in liver cancer using an integrative oncogenomic approach. *Cell*. 2006;125(7):1253-67.  
429 6. Ma O, Cai WW, Zender L, Dayaram T, Shen J, Herron AJ, et al. MMP13, Birc2 (cIAP1), and Birc3 (cIAP2),  
430 amplified on chromosome 9, collaborate with p53 deficiency in mouse osteosarcoma progression. *Cancer Res*.  
431 2009;69(6):2559-67.  
432 7. Cheng L, Zhou Z, Flesken-Nikitin A, Toshkov IA, Wang W, Camps J, et al. Rb inactivation accelerates neoplastic  
433 growth and substitutes for recurrent amplification of cIAP1, cIAP2 and Yap1 in sporadic mammary carcinoma  
434 associated with p53 deficiency. *Oncogene*. 2010;29(42):5700-11.  
435 8. Jin J, Xiao Y, Hu H, Zou Q, Li Y, Gao Y, et al. Proinflammatory TLR signalling is regulated by a TRAF2-dependent  
436 proteolysis mechanism in macrophages. *Nat Commun*. 2015;6:5930.  
437 9. Yin Q, Lamothe B, Darnay BG, Wu H. Structural basis for the lack of E2 interaction in the RING domain of TRAF2.  
438 *Biochemistry*. 2009;48(44):10558-67.  
439 10. Dhillon B, Aleithan F, Abdul-Sater Z, Abdul-Sater AA. The Evolving Role of TRAFs in Mediating Inflammatory  
440 Responses. *Front Immunol*. 2019;10:104.  
441 11. Marivin A, Berthelet J, Cartier J, Paul C, Gemble S, Morizot A, et al. cIAP1 regulates TNF-mediated cdc42  
442 activation and filopodia formation. *Oncogene*. 2014;33(48):5534-45.

- 443 12. Vischioni B, Giaccone G, Span SW, Kruyt FA, Rodriguez JA. Nuclear shuttling and TRAF2-mediated retention in  
444 the cytoplasm regulate the subcellular localization of cIAP1 and cIAP2. *Exp Cell Res.* 2004;298(2):535-48.
- 445 13. Zhou AY, Shen RR, Kim E, Lock YJ, Xu M, Chen ZJ, et al. IKKepsilon-mediated tumorigenesis requires K63-linked  
446 polyubiquitination by a cIAP1/cIAP2/TRAF2 E3 ubiquitin ligase complex. *Cell reports.* 2013;3(3):724-33.
- 447 14. Dupoux A, Cartier J, Cathelin S, Filomenko R, Solary E, Dubrez-Daloz L. cIAP1-dependent TRAF2 degradation  
448 regulates the differentiation of monocytes into macrophages and their response to CD40 ligand. *Blood.*  
449 2009;113(1):175-85.
- 450 15. Kreckel J, Anany MA, Siegmund D, Wajant H. TRAF2 Controls Death Receptor-Induced Caspase-8 Processing  
451 and Facilitates Proinflammatory Signaling. *Front Immunol.* 2019;10:2024.
- 452 16. Mace PD, Smits C, Vaux DL, Silke J, Day CL. Asymmetric recruitment of cIAPs by TRAF2. *J Mol Biol.*  
453 2010;400(1):8-15.
- 454 17. Zheng C, Kabaleeswaran V, Wang Y, Cheng G, Wu H. Crystal structures of the TRAF2: cIAP2 and the TRAF1:  
455 TRAF2: cIAP2 complexes: affinity, specificity, and regulation. *Mol Cell.* 2010;38(1):101-13.
- 456 18. Baud V, Liu ZG, Bennett B, Suzuki N, Xia Y, Karin M. Signaling by proinflammatory cytokines: oligomerization  
457 of TRAF2 and TRAF6 is sufficient for JNK and IKK activation and target gene induction via an amino-terminal effector  
458 domain. *Genes Dev.* 1999;13(10):1297-308.
- 459 19. Tang Z, Li C, Kang B, Gao G, Zhang Z. GEPIA: a web server for cancer and normal gene expression profiling and  
460 interactive analyses. *Nucleic Acids Res.* 2017;45(W1):W98-W102.
- 461 20. Csomos RA, Brady GF, Duckett CS. Enhanced cytoprotective effects of the inhibitor of apoptosis protein cellular  
462 IAP1 through stabilization with TRAF2. *J Biol Chem.* 2009;284(31):20531-9.
- 463 21. Vallabhapurapu S, Matsuzawa A, Zhang W, Tseng PH, Keats JJ, Wang H, et al. Nonredundant and  
464 complementary functions of TRAF2 and TRAF3 in a ubiquitination cascade that activates NIK-dependent alternative  
465 NF-kappaB signaling. *Nat Immunol.* 2008;9(12):1364-70.
- 466 22. Li X, Yang Y, Ashwell JD. TNF-RII and c-IAP1 mediate ubiquitination and degradation of TRAF2. *Nature.*  
467 2002;416(6878):345-7.
- 468 23. Matsuzawa A, Tseng PH, Vallabhapurapu S, Luo JL, Zhang W, Wang H, et al. Essential cytoplasmic translocation  
469 of a cytokine receptor-assembled signaling complex. *Science.* 2008;321(5889):663-8.
- 470 24. Shu HB, Takeuchi M, Goeddel DV. The tumor necrosis factor receptor 2 signal transducers TRAF2 and c-IAP1  
471 are components of the tumor necrosis factor receptor 1 signaling complex. *Proc Natl Acad Sci U S A.*  
472 1996;93(24):13973-8.
- 473 25. Borghi A, Verstrepen L, Beyaert R. TRAF2 multitasking in TNF receptor-induced signaling to NF- $\kappa$ B, MAP kinases  
474 and cell death. *Biochem Pharmacol.* 2016;116:1-10.
- 475 26. Ceccarelli A, Di Venere A, Nicolai E, De Luca A, Minicozzi V, Rosato N, et al. TNFR-Associated Factor-2 (TRAF2):  
476 Not Only a Trimer. *Biochemistry.* 2015;54(40):6153-61.
- 477 27. Ye H, Park YC, Kreishman M, Kieff E, Wu H. The structural basis for the recognition of diverse receptor  
478 sequences by TRAF2. *Mol Cell.* 1999;4(3):321-30.
- 479 28. Park HH. Structure of TRAF Family: Current Understanding of Receptor Recognition. *Front Immunol.*  
480 2018;9:1999.
- 481 29. Peng C, Zhu F, Wen W, Yao K, Li S, Zykova T, et al. Tumor necrosis factor receptor-associated factor family  
482 protein 2 is a key mediator of the epidermal growth factor-induced ribosomal S6 kinase 2/cAMP-responsive element-  
483 binding protein/Fos protein signaling pathway. *J Biol Chem.* 2012;287(31):25881-92.
- 484 30. Dubrez L, Berthelet J, Glorian V. IAP proteins as targets for drug development in oncology. *OncoTargets and*  
485 *therapy.* 2013;9:1285-304.
- 486 31. Park MH, Hong JT. Roles of NF- $\kappa$ B in Cancer and Inflammatory Diseases and Their Therapeutic Approaches.  
487 *Cells.* 2016;5(2).
- 488 32. Vu NT, Park MA, Shultz MD, Bulut GB, Ladd AC, Chalfant CE. Caspase-9b Interacts Directly with cIAP1 to Drive  
489 Agonist-Independent Activation of NF- $\kappa$ B and Lung Tumorigenesis. *Cancer Res.* 2016;76(10):2977-89.
- 490 33. Xu L, Zhu J, Hu X, Zhu H, Kim HT, LaBaer J, et al. c-IAP1 cooperates with Myc by acting as a ubiquitin ligase for  
491 Mad1. *Mol Cell.* 2007;28(5):914-22.
- 492 34. Li H, Fang Y, Niu C, Cao H, Mi T, Zhu H, et al. Inhibition of cIAP1 as a strategy for targeting c-MYC-driven  
493 oncogenic activity. *Proc Natl Acad Sci U S A.* 2018;115(40):E9317-E24.
- 494 35. Bishop GA, Abdul-Sater AA, Watts TH. Editorial: TRAF Proteins in Health and Disease. *Front Immunol.*  
495 2019;10:326.
- 496 36. Sondarva G, Kundu CN, Mehrotra S, Mishra R, Rangasamy V, Sathyanarayana P, et al. TRAF2-MLK3 interaction  
497 is essential for TNF-alpha-induced MLK3 activation. *Cell Res.* 2010;20(1):89-98.

- 498 37. Korchnak AC, Zhan Y, Aguilar MT, Chadee DN. Cytokine-induced activation of mixed lineage kinase 3 requires  
499 TRAF2 and TRAF6. *Cell Signal*. 2009;21(11):1620-5.
- 500 38. Zhao Y, Conze DB, Hanover JA, Ashwell JD. Tumor necrosis factor receptor 2 signaling induces selective c-IAP1-  
501 dependent ASK1 ubiquitination and terminates mitogen-activated protein kinase signaling. *J Biol Chem*.  
502 2007;282(11):7777-82.
- 503 39. Nishitoh H, Saitoh M, Mochida Y, Takeda K, Nakano H, Rothe M, et al. ASK1 is essential for JNK/SAPK activation  
504 by TRAF2. *Mol Cell*. 1998;2(3):389-95.
- 505 40. Chadee DN, Yuasa T, Kyriakis JM. Direct activation of mitogen-activated protein kinase kinase kinase MEKK1  
506 by the Ste20p homologue GCK and the adapter protein TRAF2. *Mol Cell Biol*. 2002;22(3):737-49.
- 507 41. Annibaldi A, Meier P. Checkpoints in TNF-Induced Cell Death: Implications in Inflammation and Cancer. *Trends*  
508 *Mol Med*. 2018;24(1):49-65.
- 509 42. Dogan T, Harms GS, Hekman M, Karreman C, Oberoi TK, Alnemri ES, et al. X-linked and cellular IAPs modulate  
510 the stability of C-RAF kinase and cell motility. *Nat Cell Biol*. 2008;10(12):1447-55.
- 511 43. Zarnegar BJ, Wang Y, Mahoney DJ, Dempsey PW, Cheung HH, He J, et al. Noncanonical NF-kappaB activation  
512 requires coordinated assembly of a regulatory complex of the adaptors cIAP1, cIAP2, TRAF2 and TRAF3 and the kinase  
513 NIK. *Nature immunology*. 2008;9(12):1371-8.
- 514 44. Johnson DE, O'Keefe RA, Grandis JR. Targeting the IL-6/JAK/STAT3 signalling axis in cancer. *Nat Rev Clin Oncol*.  
515 2018;15(4):234-48.
- 516 45. Zhu S, Jin J, Gokhale S, Lu AM, Shan H, Feng J, et al. Genetic Alterations of TRAF Proteins in Human Cancers.  
517 *Front Immunol*. 2018;9:2111.
- 518 46. Didelot C, Lanneau D, Brunet M, Bouchot A, Cartier J, Jacquelin A, et al. Interaction of heat-shock protein 90 beta  
519 isoform (HSP90 beta) with cellular inhibitor of apoptosis 1 (c-IAP1) is required for cell differentiation. *Cell Death Differ*.  
520 2008;15(5):859-66.
- 521 47. Pathan M, Keerthikumar S, Ang CS, Gangoda L, Quek CY, Williamson NA, et al. FunRich: An open access  
522 standalone functional enrichment and interaction network analysis tool. *Proteomics*. 2015;15(15):2597-601.

523

524 **Figure legends**

525

526 **Figure 1. TRAF2 binding is critical for the oncogenic activity of cIAP1.** Wild type (wt), cIAP1<sup>-/-</sup> (SKO) or cIAP1<sup>-/-</sup>/cIAP2<sup>-/-</sup> (DKO) mouse embryonic fibroblasts (MEFs) were transformed by Hras-V12 oncogene and reconstituted with cIAP1, or cIAP1 mutants cIAP1<sup>ΔBIR1</sup> (ΔBIR1), cIAP1<sup>L47A</sup> (L47A) or cIAP1<sup>ΔBIR2</sup> (ΔBIR2). **A, D, F.** Western blot analysis of cIAPs and Ras. HSC70 was used as loading control. **B, E, G.** Cells (500 000) were injected subcutaneously in nude NMRI mice. Tumor size was measured every two days (B), 17 (E) or 3 weeks (G) post-injection. Statistical analyses were performed using the Mann Whitney test. Mean ± SEM (B) or Mean ± SD (E, G), n=10-30. In B, the statistical analyses compared SKO or DKO with cIAP1-expressing SKO or DKO respectively. **C, H.** Cells (10<sup>6</sup>) were injected in the caudal vein in nude NMRI mice. The number of lung foci was determined 36 days after intravenous injection. Statistical analyses were performed using the Mann Whitney test. Mean ± SD, n=8-20. **I.** Clonogenic growth of cells in soft agar medium. Statistical analyses were performed using the Wilcoxon test. Mean ± SD, n=3-5.

536

537 **Figure 2. Forced clustering of TRAF2 stimulated tumor growth, independently of cIAP1.** cIAP1, cIAP1<sup>ΔBIR1</sup> or the isolated cIAP1-BIR1 domain (iBIR1) were expressed in HRas-V12-transformed DKO MEFs. **A.** Immunofluorescence analysis of TRAF2 in DKO, DKO-cIAP1, DKO-cIAP1<sup>ΔBIR1</sup> (ΔBIR1) or DKO-iBIR1. Scale bars: 10μm. **B.** Immunofluorescence analysis of TRAF2 and indicated organelle markers in DKO-cIAP1. Scale bars: 7μm. **C.** Western blot analysis of cIAP1. β-actin was used as loading control. **D.** Colonies formed in soft-agar medium. Scale bars: 100μm. **E.** DKO, DKO-cIAP1 and DKO-iBIR1 MEFs (500 000) were subcutaneously injected into nude mice. Tumor volume 24 days after injection is represented. Statistical analyses comparing the DKO group and cIAP1 or iBIR1-expressing group were performed using the Mann Whitney test. Mean ± SEM, n=12-13.

545 **Figure 3. TRAF2 interactome.** A549 cells were incubated for 6 hours with vehicle (NT) or 5μM GDC-0152 (GDC).

546 TRAF2 was immunoprecipitated and its interactome was analyzed by ESI-TRAP mass spectrometry. Analysis was performed using the functional enrichment analysis tool (FunRich) using the FunRich (B, F) or UniProt (D, E)

548 databases. **A.** Western blot analysis of cIAP1, cIAP2, XIAP and TRAF2. HSC70 was used as loading control. **B, F.**

549 Number of partners of TRAF2 in untreated (NT) or GDC-0152-treated cells. Mean ± SD, n=3 (NT) or 2 (GDC-0152). **C.**

550 Peptides identified by mass spectrometry after TRAF2 immunoprecipitation. **D, E.** Enrichment of TRAF2 partners in

551 subcellular compartments (D) and biological processes (E). Mean  $\pm$  SD, n=3 (NT) or 2 (GDC-0152). F. Venn diagram.  
552 One representative experiment is shown.

553

554 **Figure 4. TRAF2 binding is essential for the activation of the canonical NF- $\kappa$ B and ERK1/2 signaling pathways. A.**  
555 Western blot analysis of proteins involved in the canonical NF- $\kappa$ B, p38-MAPK, ERK1/2 and JNK signaling pathways.  $\beta$ -  
556 actin or HSC70 were used as loading control. **B.** NF- $\kappa$ B target genes were analyzed in MEF DKO-clAP1 and DKO-  
557 clAP1 <sup>$\Delta$ BIR1</sup> by RT-qPCR array (Qiagen NF $\kappa$ B Signaling Pathway RT2 Profiler PCR Array). **C.** Western blot analysis of the  
558 NF- $\kappa$ B p52 subunit in cytoplasmic and nuclear-enriched fractions. XIAP was used as cytoplasmic fraction control and  
559 HSC70 as a loading control.

560

561 **Figure 5. clAP1 and TRAF2 are critical for the activation of the JAK/STAT3 signaling pathways. A.** Western blot  
562 analysis of the proteins involved in the JAK/STAT3 signaling pathway in MEF DKO expressing clAP1, clAP1 <sup>$\Delta$ BIR1</sup> or  
563 clAP1<sup>L47A</sup>. HSC70 is used as loading control **B.** p-STAT3 was quantified using the Image J software. Mann-Whitney  
564 statistical analysis, mean  $\pm$  SD of 3 independent experiments is shown. **C.** MEFs were transfected with TRAF2-  
565 targeting siRNAs. TRAF2 and STAT3 phosphorylation were analyzed by western blot.  $\beta$ -actin was used as loading  
566 control. Sc: scramble siRNA. **D.** clAP1-expressing DKO MEFs (DKO-clAP1) were treated for 4hrs with 2 $\mu$ M Bay-11-  
567 7082, 2 $\mu$ M trametinib or 2 $\mu$ M niclosamide. Western blot analysis of indicated proteins. HSC70 is used as loading  
568 control. **E.** RT-qPCR analysis of IL-6 mRNA level in MEFs DKO, DKO-clAP1 and DKO-clAP1 <sup>$\Delta$ BIR1</sup> or DKO-clAP1 treated for  
569 4 hrs with 2 $\mu$ M Bay-11-7082 or 2 $\mu$ M trametinib. Mann Whitney test. Mean  $\pm$  SD, n=3. **F.** Western blot analysis of the  
570 phosphorylation of STAT3 in DKO and DKO-clAP1 MEFs incubated in the presence of neutralizing anti-IL-6 antibody  
571 (100ng/mL) for 24hrs. **G.** Correlative analysis of the expression of *IL6* and clAP1-encoding *BIRC2* genes in lung  
572 adenocarcinoma (LUAD), breast invasive carcinoma (BRCA) and thyroid carcinoma (THCA) using the publicly available  
573 TCGA dataset and gene expression profiling interactive analysis (GEPIA) tools. **H, I.** Western blot analysis of the  
574 proteins involved in the JAK2/STAT3 signaling pathway in A549 lung carcinoma cells transfected with siRNAs directed  
575 against clAP1 or TRAF2 (H) or treated for 6 hours with the indicated concentration of the smac mimetic GDC-0152 (I).  
576 HSC70 was used as loading control.

577

578 **Figure 6. STAT3 signaling pathway is required for cIAP1-mediated tumor cell growth.**

579 **A-D.** DKO-cIAP1 or DKO cIAP1<sup>ΔBIR</sup> MEFs (750 000) were subcutaneously injected into nude mice. When the tumor  
580 reached 100 mm<sup>3</sup> (indicated by the narrow), mice were daily treated by intraperitoneal injection of vehicle (NT group)  
581 or 30 mg/Kg niclosamide (**A, B**) or 1mg/kg trametinib (**C, D**). Tumor size was measured every two days (**A, C**) or 25-26  
582 days after cell challenge (**B, D**). The results of the statistical analyzes comparing the vehicle with niclosamide or  
583 trametinib-treated DKO-cIAP1 mice groups are indicated above the graphs while those comparing vehicle with  
584 niclosamide or trametinib-treated DKO cIAP1<sup>ΔBIR</sup> are indicated below. Mann Whitney test, mean ± SEM (A,C) or mean  
585 ± SD (B,D) , n=12-14. **E.** Clonogenic growth of DKO-cIAP1 and DKO-cIAP1<sup>ΔBIR1</sup> MEFs incubated in the presence of vehicle  
586 (0) or indicated concentrations of niclosamide. The Wilcoxon test was used for statistical analysis, Mean ± SD, n=3. **F,**  
587 **G.** DKO or cIAP1-expressing DKO MEFs were transfected with control (Ctl) or STAT3-directed siRNAs (#1, #2). Western  
588 blot analysis of STAT3 (**F**) and cell count 72hrs after transfection (**G**). The Wilcoxon test was used for statistical analysis,  
589 Mean ± SD, n=3.

**FIGURE 1**

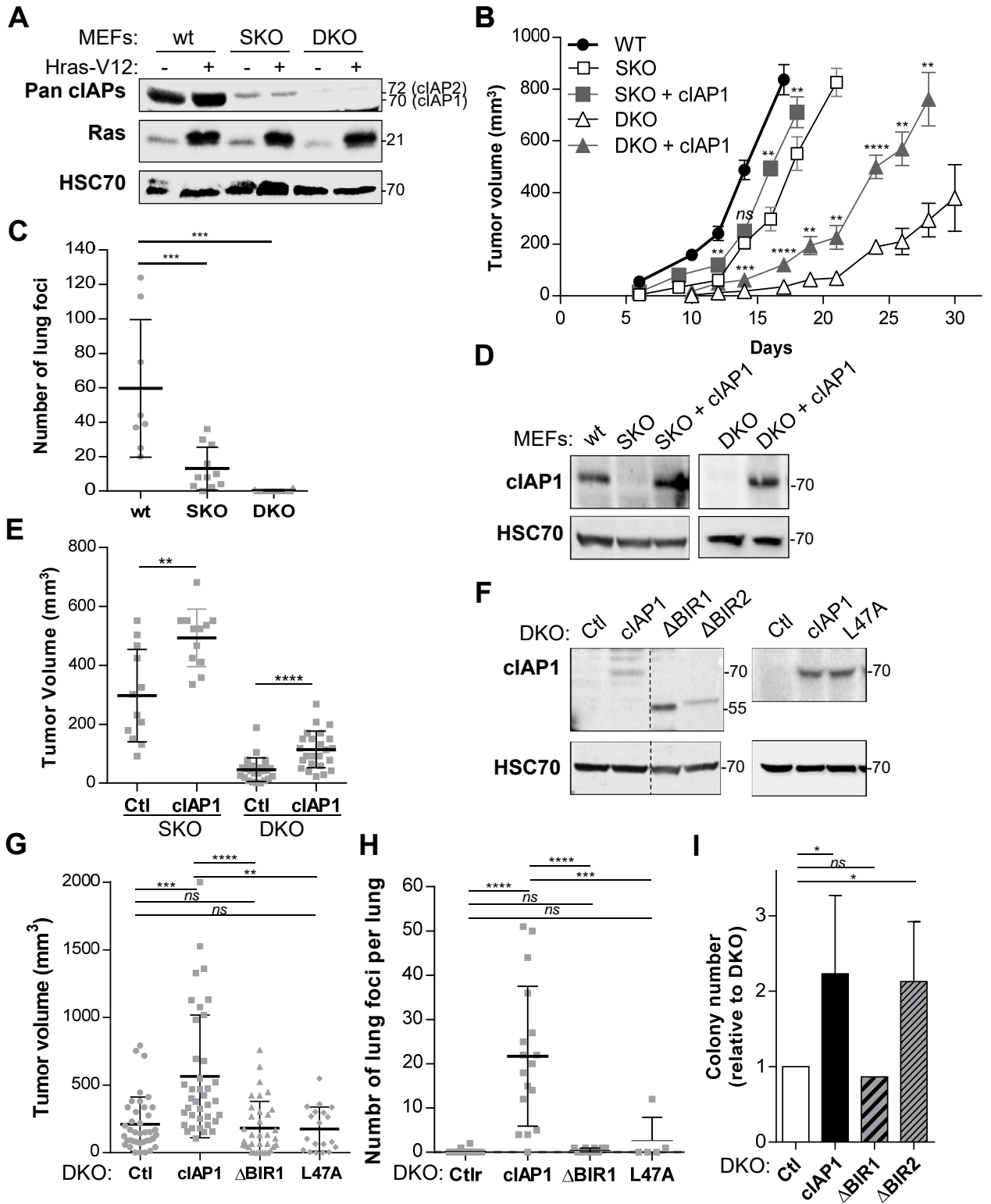


**FIGURE 2**

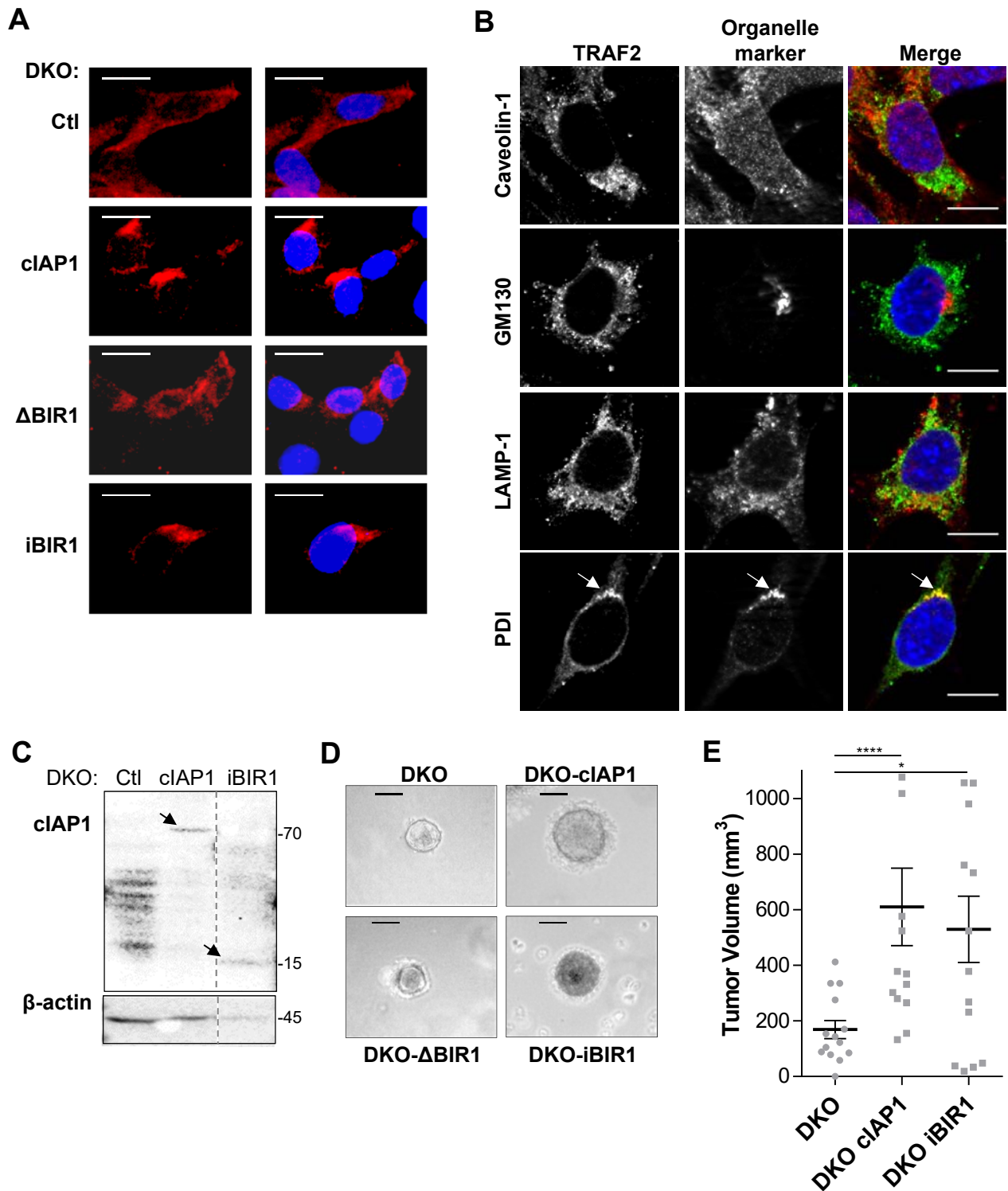


# FIGURE 3

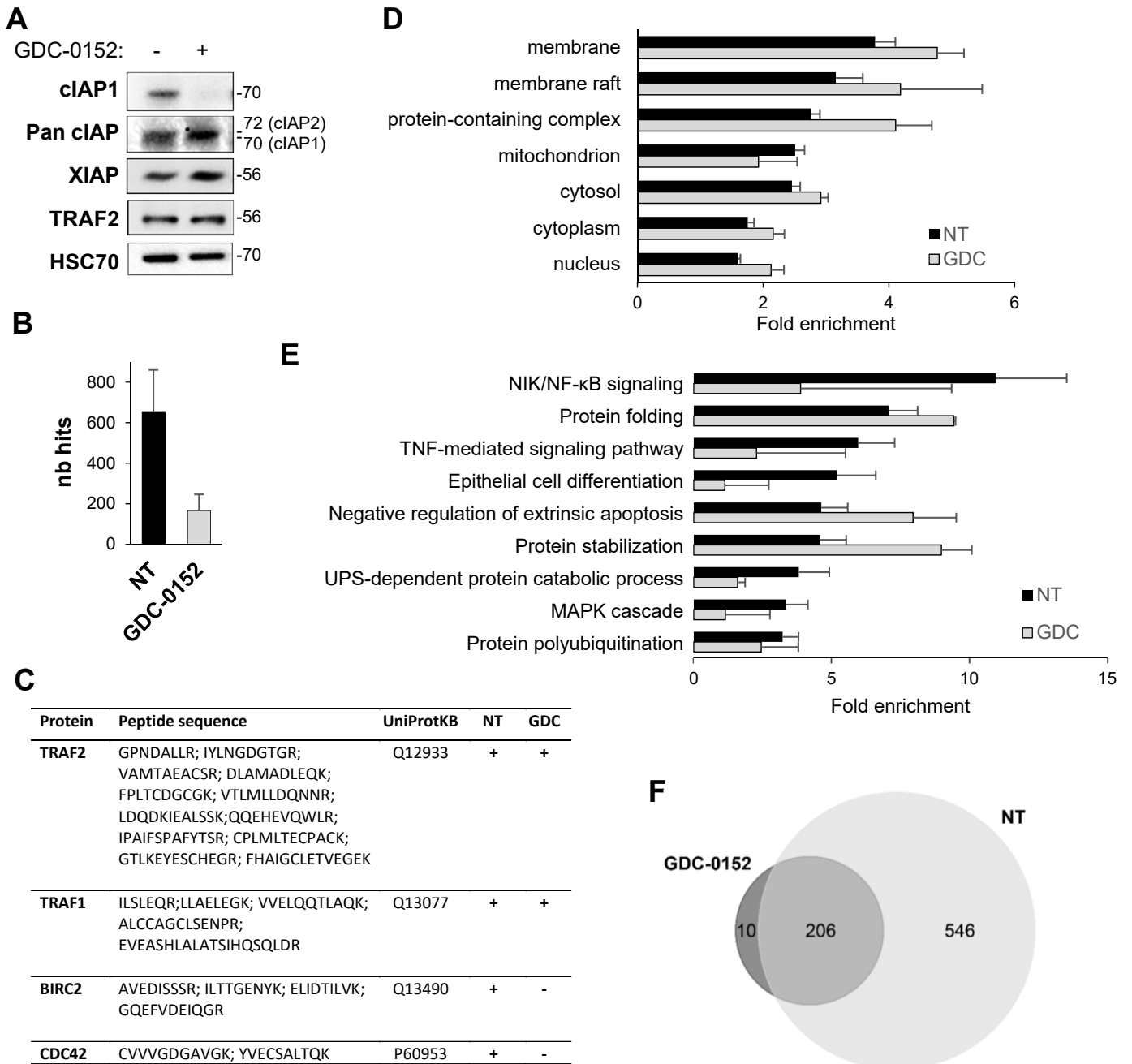


**FIGURE 4**

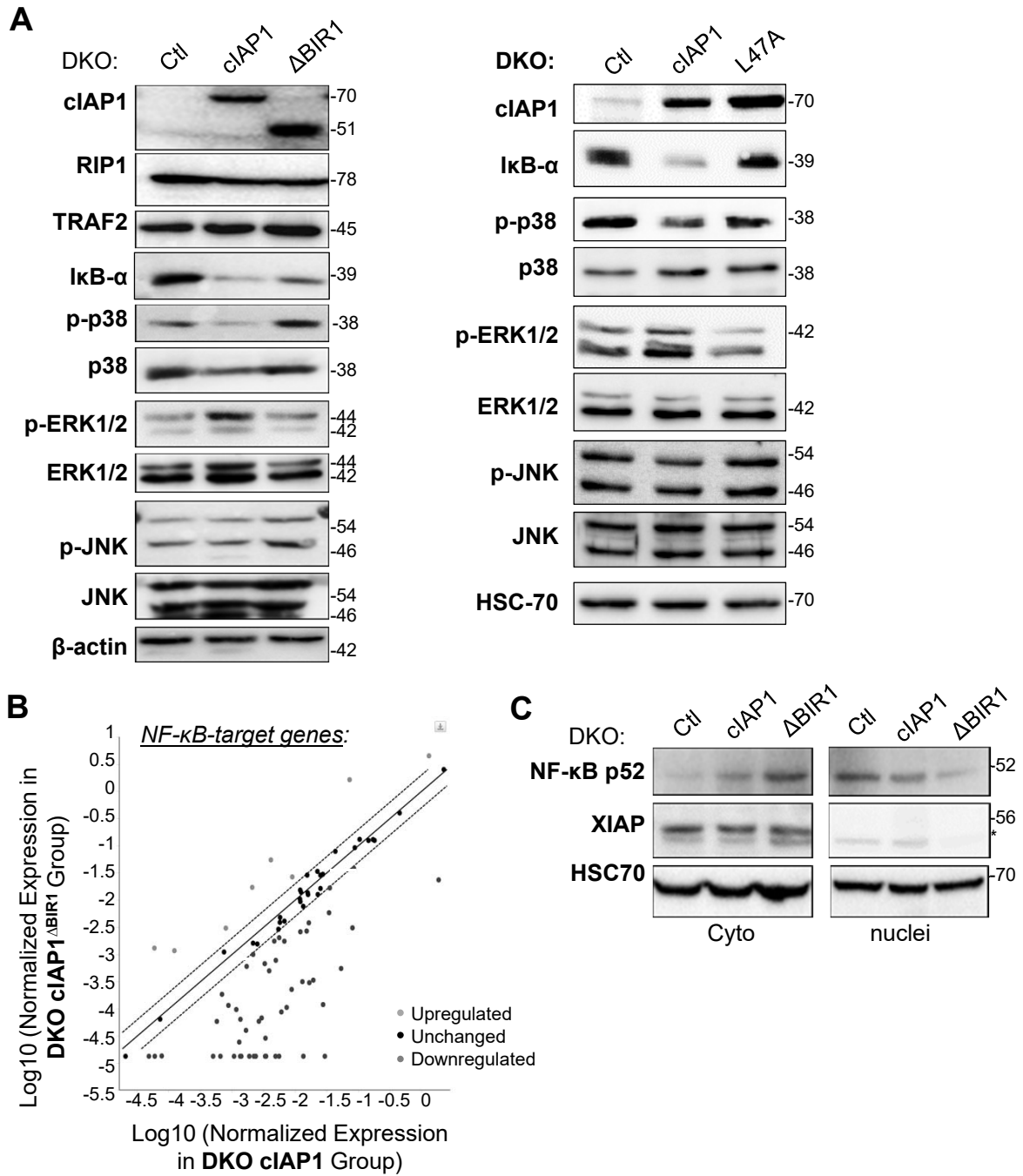


**FIGURE 5**

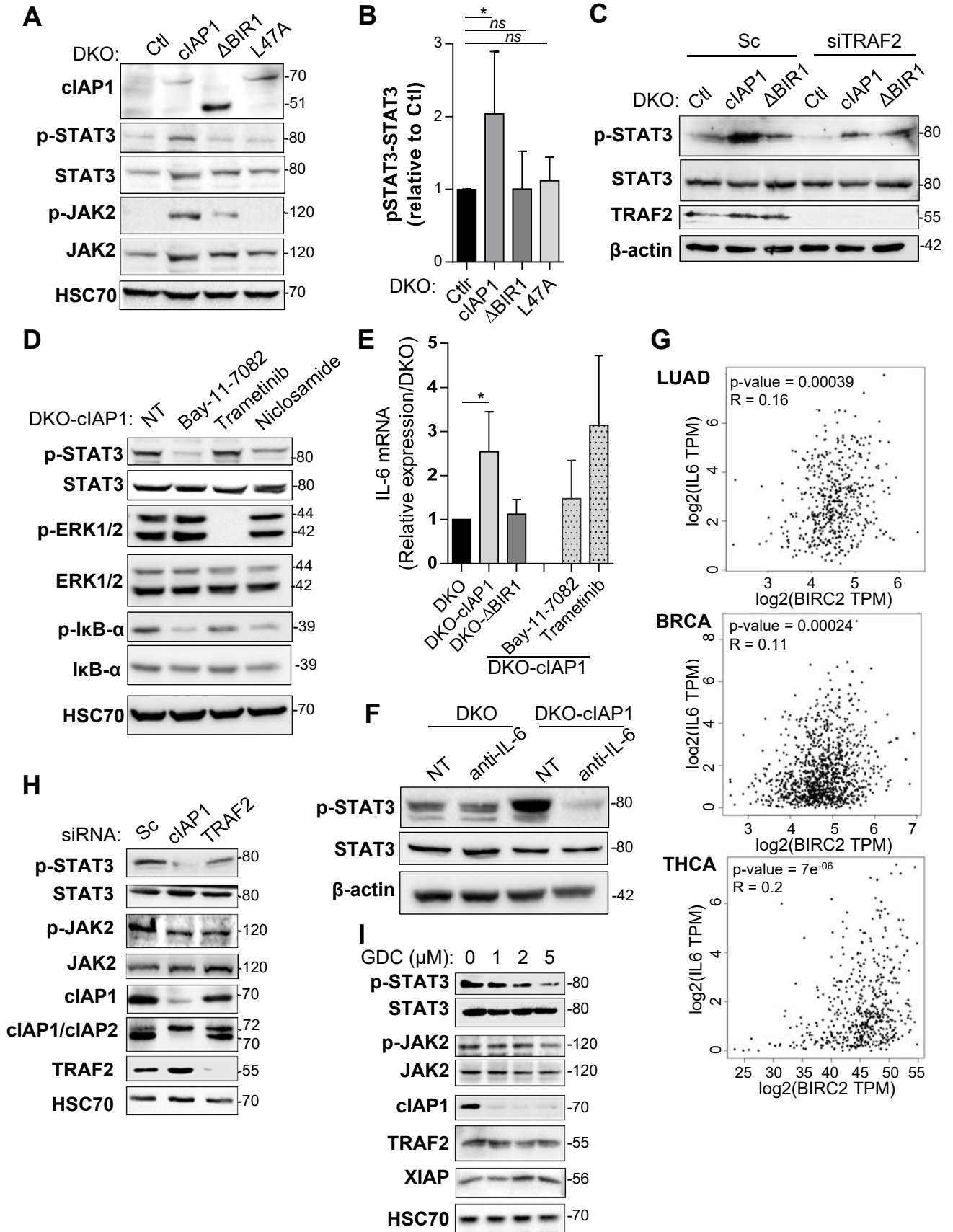


**FIGURE 6**

